[CANCER RESEARCH 64, 7977–7984, November 1, 2004]

Tumor Cell and Endothelial Cell Therapy of Oral Cancer by Dual Tyrosine Kinase Receptor Blockade

Orhan G. Yigitbasi,[1] Maher N. Younes,[1] Dao Doan,[1] Samar A. Jasser,[1] Bradley A. Schiff,[1] Corazon D. Bucana,[2] Benjamin N. Bekele,[3] Isaiah J. Fidler,[2] and Jeffrey N. Myers[1,2]

Departments of [1]Head and Neck Surgery, [2]Cancer Biology, and [3]Biostatistics, The University of Texas M. D. Anderson Cancer Center, Houston, Texas

ABSTRACT

Expression of the epidermal growth factor (EGF) and activation of its receptor (EGFR), a tyrosine kinase, are associated with progressive growth of head and neck cancer. Expression of the vascular endothelial growth factor (VEGF) is associated with angiogenesis and progressive growth of tumor. The tyrosine kinase inhibitor NVP-AEE788 (AEE788) blocks the EGF and VEGF signaling pathways. We examined the effects of AEE788 administered alone, or with paclitaxel (Taxol), on the progression of human head and neck cancer implanted orthotopically into nude mice. Cells of two different human oral cancer lines, JMAR and MDA1986, were injected into the tongues of nude mice. Mice with established tumors were randomized to receive three times per week oral AEE788, once weekly injected paclitaxel, AEE788 plus paclitaxel, or placebo. Oral tumors were resected at necropsy. Kinase activity, cell proliferation, apoptosis, and mean vessel density were determined by immunohistochemical immunofluorescent staining. AEE788 inhibited cell growth, induced apoptosis, and reduced the phosphorylation of EGFR, VEGFR-2, AKT, and mitogen-activated protein kinase in both cell lines. Mice treated with AEE788 and AEE788 plus paclitaxel had decreased microvessel density, decreased proliferative index, and increased apoptosis. Hence, AEE788 inhibited tumor vascularization and growth and prolonged survival. Inhibition of EGFR and VEGFR phosphorylation by AEE788 effectively inhibits cellular proliferation of squamous cell carcinoma of the head and neck, induces apoptosis of tumor endothelial cells and tumor cells, and is well tolerated in mice. These data recommend the consideration of patients with head and neck cancer for inclusion in clinical trials of AEE788.

INTRODUCTION

Squamous cell carcinoma of the head and neck (SCCHN) is the sixth most common human neoplasm, with an estimated annual worldwide incidence of 500,000 new cases (1, 2). Despite developments in surgery, chemotherapy, radiotherapy, and combinations of treatment modalities, the long-term survival of patients with SCCHN has remained ~50% for the past 30 years (3). To improve the outcome for patients with SCCHN, novel therapeutic approaches are needed.

The epidermal growth factor receptor (EGFR) is a tyrosine kinase receptor of the ErbB family that is expressed or highly expressed in a range of solid tumors, including head and neck cancers (4). EGFR activation induces activation of several downstream intracellular substrates, leading to mitogenic signaling and other tumor-promoting cellular activities (5). In human tumors, overexpression of this receptor correlates with a more aggressive clinical course (4).

Nevertheless, recent experimental evidence suggests that the cancer cells can escape from growth inhibition by using alternative growth pathways or by constitutive activation of downstream signaling effectors. For example, human A431 cancer cells xenografts can acquire resistance to anti-EGFR monoclonal antibodies (mAbs), such as C225 and hR3, by increased tumor-induced angiogenesis due to the constitutive overexpression of proangiogenic growth factors, such as vascular endothelial growth factor (VEGF; ref. 6).

VEGF, a mitogen specific for vascular endothelial cells, is considered to play a key role in angiogenic processes (7). VEGF binds to two distinct receptors on endothelial cells, flt-1 (VEGFR-1) and flk-1/KDR receptor (VEGFR-2), the latter of which is considered the dominant signaling receptor governing endothelial cell permeability, proliferation, and differentiation (8). Expression of these receptors in normal tissues is low and is up-regulated during the development of pathological conditions associated with neovascularization (9, 10). Inhibition of VEGF-induced angiogenic signals would be expected to selectively target tumor-associated vessels because division of endothelial cells in the normal vasculature is infrequent (8). Hence, inhibition of VEGF-mediated effects likely is an attractive alternative or complement to cytotoxic therapies.

Blockade of EGFR with specific mAbs or small molecule chemical inhibitors has been demonstrated to decrease tumor cell production of proangiogenic molecules (such as VEGF) and to inhibit tumor-associated angiogenesis (10, 11). A recent report documented that treatment combining an anti-EGFR antibody with an anti-KDR (VEGFR-2) antibody in a murine model of human colon cancer decreased tumor vascularity and increased tumor and endothelial cell apoptosis (12). Therefore, although EGFR/ErbB2 inhibitors can inhibit production of VEGF by the tumor cells, a more potent antitumor response can be achieved through the concomitant inhibition of VEGFR. Dual inhibitors, combining both activities in the same molecule, would therefore be attractive for the treatment of numerous solid tumors.

NVP-AEE788 (AEE788; molecular weight, M_r 440,600) is an orally administered dual specific-kinase inhibitor targeting both the ErbB and VEGF receptors. It belongs to the class of the 7H-pyrrolo[2,3-d] pyrimidines. The efficacy of AEE788 *in vitro* against lung, bladder, and breast cancer cell lines has been demonstrated, and AEE788 has proved to be an effective antitumor compound in human tumor xenograft models (data on file at Novartis Pharma AG, Basel, Switzerland).

In the present study, we evaluated the therapeutic effect of the AEE788 administered alone or in combination with paclitaxel against established squamous cell carcinomas growing orthotopically within the tongue of athymic nude mice.

MATERIALS AND METHODS

JMAR and MDA1986 Cell Lines and Culture Conditions. For these studies, we used the invasive oral squamous carcinoma cell lines JMAR and MDA1986 (13). Cell lines were grown in DMEM supplemented with 10% fetal bovine serum, sodium pyruvate, nonessential amino acids, L-glutamine, and a 2-fold vitamin solution (Life Technologies, Inc., Grand Island, NY). Adherent monolayer cultures were maintained on plastic and incubated at 37°C in a mixture of 5% CO_2 and 95% air. The cultures were free of *Mycoplasma* and pathogenic murine viruses. The cultures were maintained for no longer than 12 weeks after recovery from frozen stocks.

Received 4/26/04; revised 7/29/04; accepted 8/27/04.

Grant support: National Institute of Dental and Craniofacial Research-NIH Grant R01DE01461301 and National Cancer Institute-NIH Grant P50CA097007.

The costs of publication of this article were defrayed in part by the payment of page charges. This article must therefore be hereby marked *advertisement* in accordance with 18 U.S.C. Section 1734 solely to indicate this fact.

Requests for reprints: Jeffrey N. Myers, Department of Head and Neck Surgery, Unit 441, The University of Texas M. D. Anderson Cancer Center, 1515 Holcombe Boulevard, Houston, TX 77030-4009. Phone: (713) 792-6920; Fax: (713) 794-4662; E-mail: jmyers@mdanderson.org.

Measurement of Cell Proliferation. The antiproliferative effects of AEE788 against JMAR and MDA1986 cells were determined by a 3-(4,5-dimethylthiazol-2-yl)-2,5-diphenyltetrazolium bromide (MTT) assay that measures cell proliferation based on the ability of live cells to use MTT and convert it to a dark blue formazan (14). One thousand cells were plated into each well of a 96-well tissue culture plate. The cells were grown in DMEM supplemented with sodium pyruvate, essential amino acids, and 10% FBS. After a 24-hour attachment period, the cells were refed with medium (negative control with DMEM alone) or medium containing paclitaxel. After a 3-day incubation, the number of metabolically active cells was determined by MTT assay as measured by a MR-5000 96-well microtiter plate reader (Dynatech, Inc., Chantilly, VA) at an absorbance at 570 nm. Growth inhibition was calculated using the following formula: cytostasis (%) = $[1 - (A/B)] \times 100$, where A is the absorbance of treated cells, and B is the absorbance of control cells.

Measurement of Cell Death. Cells were plated at a density of 2×10^5 cells per well in 6-well plates (Costar, Cambridge, MA) and maintained for 24 hours before treatment with AEE788 and paclitaxel. Seventy-two hours later, the extent of cell death was determined by propidium iodide (PI) staining of hypodiploid DNA (15). For the PI staining, cells were resuspended in Nicoletti buffer 50 μg/mL PI (Sigma, St. Louis, MO) and 0.1% sodium citrate for 20 minutes at 4°C. Cells were then analyzed by flow cytometry, and the sub-G_0-G_1 fraction was measured with the Lysis program (Biosciences Clontech [BD], Franklin Lakes, NJ). The percentage of cells undergoing specific apoptosis was calculated by subtracting the percentage of cells that had undergone spontaneous apoptosis in the relevant controls from the total percentage of apoptotic cells in the study cultures (16).

Western Blotting. To determine whether AEE788 acted through its purported mechanism *in vitro*, we evaluated the effect of this agent on inhibition of EGF-stimulated tyrosine phosphorylation of EGFR, VEGFR, mitogen-activated protein kinase (MAPK), and AKT in human JMAR and MDA1986 oral cancer cells. Under basal conditions in both serum-containing and serum-free media, both cells demonstrated a low level of autophosphorylation, which was enhanced after exposure to EGF for 15 minutes. These cell lines were plated onto 6-well plates at a concentration of 2×10^5 cells/well and then incubated for 24 hours. On the next day, cells were incubated with serum-free media for 24 hours. The study cultures were treated with AEE788 at concentrations ranging from 0.1 to 10 μmol/L and controls with DMSO alone for 1 hour. The cells were then activated with EGF recombinant (40 ng/mL) for 15 minutes, washed with PBS, scraped with lysis buffer [1% Triton X-100, 20 mmol/L Tris (pH 8.0), 137 mmol/L NaCl, 10% glycerol (v/v), 2 mmol/L EDTA, 1-mmol/L phenylmethylsulfonyl fluoride, 20 μmol/L aprotinin-leupeptin-trypsin inhibitor, and 2 mmol/L sodium orthovanadate], and centrifuged to remove insoluble protein. The samples were diluted in sample buffer [0.5 mmol/L Tris-HCl (pH 6.8), 10% SDS, 1 mol/L DTT, 10% (v/v) glycerol, and 1% bromphenol blue] and boiled. The proteins (100 μg per lane) were resolved on 10% SDS- PAGE and transferred onto 0.45-mm polyvinylidene difluoride membranes, which then were blocked with 5% (w/v) nonfat milk in 0.1% Tween 20 (v/v) in TBS (TBS-T) for 1 hour. The membrane was probed with anti-EGFR (1:3000 dilution) and anti-phospho-EGFR (Tyr^{1068}; 1:2000 dilution) antibodies, respectively, incubated overnight in 1% milk TBST, washed three times with 1× TBS-1, and incubated for 1 hour at room temperature with horseradish peroxidase-conjugated sheep antirabbit immunoglobulin (1:2000; Amersham, Inc., Arlington Heights, IL) in 1% nonfat milk. The blots were also probed with anti-phosphorylated AKT-Ser^{473} (Cell Signaling Technology, Beverly, MA), diluted 1:2000 in 1% nonfat milk TBST, phospho-MAPK ($Tyr^{42/44}$), and phospho-VEGFR-2 (pY1045), and incubated with peroxidase-conjugated donkey antirabbit IgG (1:3000; Sigma) in 1% nonfat milk. Finally, all blots were probed with anti-β-actin (1:3000; Sigma) in 1% nonfat milk, followed by horseradish peroxidase-conjugated donkey antirabbit IgG (1:4000; Amersham, Inc.) in 1% nonfat milk. Protein bands were visualized by the enhanced chemiluminescence detection system (Amersham, Inc.; ref. 16).

Reagents. For *in vivo* administration, AEE788 was dissolved and administered to mice at a concentration of 50 mg/kg three times a week. Paclitaxel was obtained from Sigma and administered at 200 μg/week. The following antibodies were used: polyclonal rabbit anti-EGF, anti-VEGF, anti-EGFR, anti-VEGFR-2, and anti-activated EGFR (Santa Cruz Biotechnology, Santa Cruz, CA); anti-activated VEGFR-2 (Oncogene, Cambridge, MA); anti-activated AKT and anti-activated MAPK (Cell Signaling Technology); mouse anti-proliferating cell nuclear antigen clone PC-10 (DAKO A/S, Copenhagen, Denmark); rat antimouse CD31/PECAM-1 and rat antimouse CD31 peroxidase-conjugated rat antimouse IgG1 (PharMingen, San Diego, CA); peroxidase-conjugated $F(ab')_2$ goat antirabbit IgG $F(ab')_2$, peroxidase-conjugated rat antimouse IgG $F(ab')_2$ fragment, Affinipure Fab-fragment goat antimouse IgG, peroxidase-conjugated goat antirat IgG, and Texas Red-conjugated goat antirat IgG (Jackson Research Laboratories, West Grove, CA); Alexa Fluor 594-conjugated goat antimouse IgG, Alexa Fluor 594-conjugated goat antirabbit IgG, and Alexa Fluor 488-conjugated goat antirabbit IgG (Molecular Probes, Eugene, OR); peroxidase-conjugated rat antimouse IgG2a (Serotec; Harlan Bioproducts for Science, Inc., Indianapolis, IN); horseradish peroxidase-conjugated donkey antirabbit IgG (Amersham, Inc.); and sheep antimouse and human IgG (Sigma). Other reagents were Hoechst Dye 3342 MW 615.9 (Hoechst, Warrington, PA), stable 3,3′-diaminobenzidine (Research Genetics, Huntsville, AL), 3-amino-9-ethylcarbazole AEC (Biogenex Laboratories, San Ramon, CA), and Gill's hematoxylin (Sigma). Prolong solution was purchased from Molecular Probes and pepsin from Biomeda (Foster City, CA).

PI and MTT were both purchased from Sigma. Stock solutions were prepared by dissolving 1 mg of each compound in 1 mL of PBS and filtering the solution to remove particles. The solution was protected from light, stored at 4°C, and used within 1 month. The enhanced chemiluminescence detection system was purchased from Amersham, and terminal deoxynucleotidyl transferase-mediated nick end labeling (TUNEL) assay was done with a commercial apoptosis detection kit (Promega, Madison, WI) with modifications as described below.

Animals and Maintenance. Male athymic nude mice (NCI-nu), ages 8 to 12 weeks, were purchased from the Animal Production Area of the National Cancer Institute-Frederick Cancer Research and Development Center (Frederick, MD). The mice were housed and maintained in laminar flow cabinets under specific pathogen-free conditions in facilities approved by the American Association for Accreditation of Laboratory Animal Care and in accordance with current regulations and standards of the United States Department of Agriculture, United States Department of Health and Human Services, and the NIH. The mice were used in accordance with Animal Care and Use Guidelines of The University of Texas M. D. Anderson Cancer Center under a protocol approved by the Institutional Animal Care Use Committee.

Orthotopic Injections of Oral Tumors. To produce tongue tumors, JMAR and MDA1986 cells were harvested from subconfluent cultures. The cells were resuspended in HBSS. Only suspensions consisting of single cells with >90% viability were used for the injections. A total number of 2×10^5 cells were resuspended in 50 μL of HBSS and injected into the tongue with a 30-gauge hypodermic needle and a tuberculin syringe as described previously (17).

Once per week, the mice were weighed, and tongue tumors were measured with microcalipers. Tumor volume was calculated using the formula $V = (A)(B^2)\pi/6$, where A is the length of the longest dimension of the tumor, and B is the length of the tumor perpendicular to A. Mice were monitored for 42 days. Mice were killed after >25% loss of the recorded initial body weight in this period, and the others were killed on day 42, after which, the body weight was determined and recorded. The tongues with tumors were resected; one half was fixed in formalin and embedded in paraffin, and the other half was embedded in OCT compound (Miles, Inc., Elkhart, IN), rapidly frozen in liquid nitrogen, and stored at −80°C. H&E staining confirmed the presence of tumor in each sample included in the analysis. Frozen and paraffin tissues were submitted for immunohistochemical analysis. Necropsy was performed in the mice to determine the extent of disease.

Therapy for Established Squamous Cell Carcinoma Tumors in Athymic Nude Mice. Mice were examined 7 days following injection of cells into the tongue. Mice with similarly sized tumors were randomized into one of four groups (n = 10 mice/group): group 1, the control group, received an oral diluent for AEE788 (90% polyethylene glycol 300 + 10% 1-methyl-2-pyrrolidinone) and i.p. HBSS; group 2, the AEE788 group, received AEE788 (50 mg/kg) by oral administration three times a week; group 3, the paclitaxel group, received paclitaxel by i.p. injection once per week (200 μg/week); and group 4, the combination therapy group, received both the oral AEE788 regimen of group 2 and the i.p. paclitaxel regimen of group 3 concomitantly.

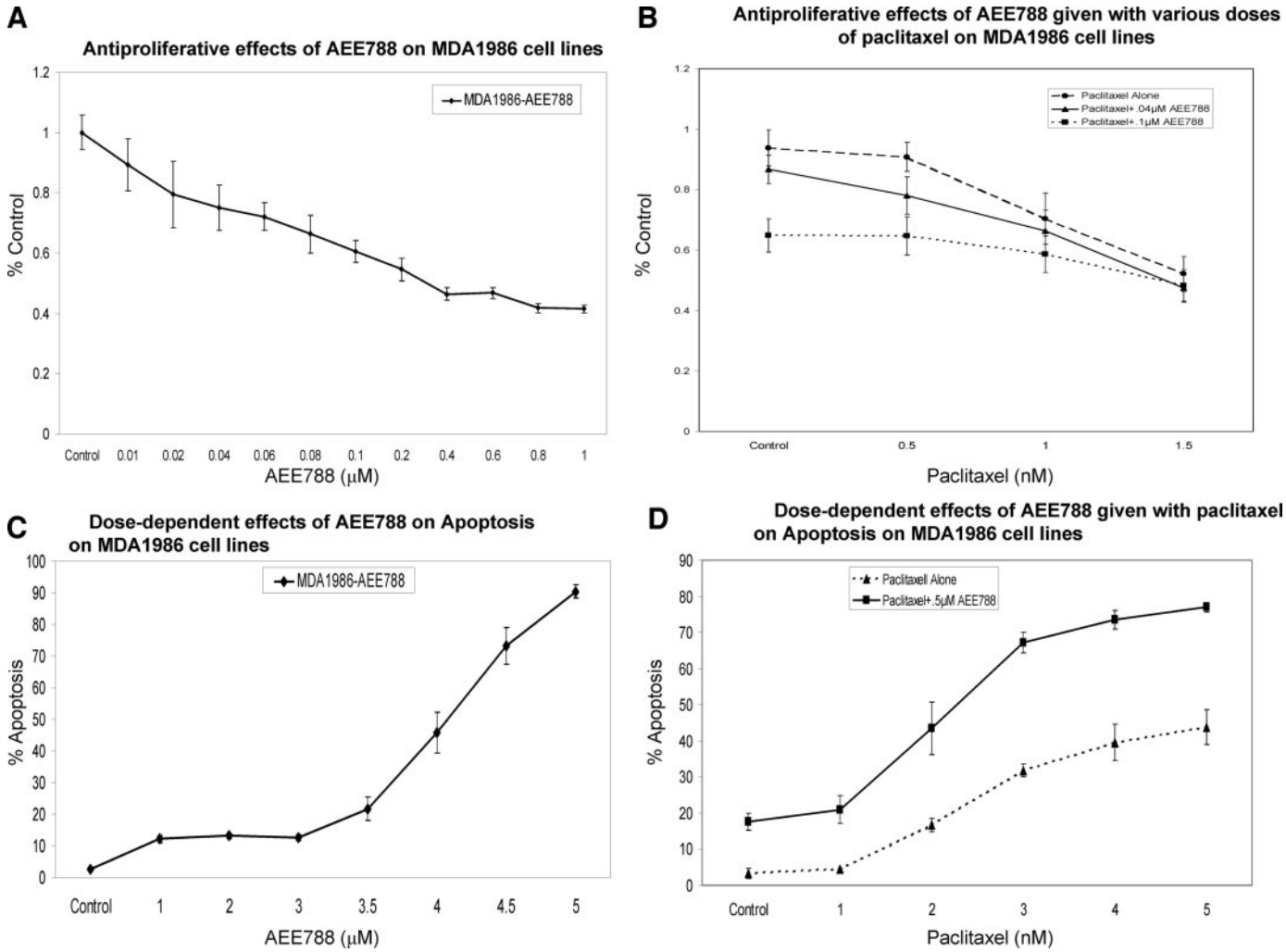

Fig. 1. Antiproliferative effects of AEE788. MTT and flow cytometric assays were performed to determine the effects of AEE788 used alone or in combination with paclitaxel on the proliferation and apoptosis of cultured MDA1986 oral cancer cells. Dose-dependent growth inhibitory effects of (*A*) AEE788 alone and (*B*) AEE788 given with various doses of paclitaxel are shown. The results shown are from a representative experiment performed in triplicate and repeated twice. AEE788 also induced apoptosis in a dose-dependent fashion; 4.5 μmol/L AEE788 were calculated to induce 50% cell death in the MDA1986 cell line after 48 hours of treatment (*C*). At 5 nmol/L concentration, paclitaxel alone induced ~45% cell death. At the same paclitaxel concentration (5 nmol/L), when 0.5 μmol/L AEE were added, the percentage of the cell death increased to 78% (*D*).

Immunohistochemical-Immunofluorescent Determination of Proliferating Cell Nuclear Antigen (PCNA), CD31/PECAM-1, EGFR, Activated EGFR, VEGFR, Activated VEGFR, Activated MAPK, and Activated AKT. Specimens of the resected tongue tumors were processed for routine histologic and immunohistochemical analyses for markers of vascularization, survival, proliferation, and cell death. *In vivo* cell proliferation and apoptosis were evaluated using anti-PCNA antibodies and the TUNEL method, respectively. Paraffin-embedded tissues were used for identification of PCNA, EGF, VEGF, EGFR, and VEGFR-2. Sections (4 to 6-μm thick) were mounted on positively charged Superfrost slides (Fisher Scientific Co., Houston, TX) and dried overnight. Sections were deparaffinized in xylene, followed by treatment with a graded series of alcohol (100, 95, and 80% etomidate /double distilled H_2O v/v) and rehydrated in PBS (pH 7.5). Sections analyzed for PCNA and VEGFR-2 were heated in a microwave oven for 5 minutes; sections analyzed for VEGF and EGFR were incubated for 20 minutes with pepsin at 37°C for antigen retrieval as described previously (18, 19).

Frozen tissues were used for identification of CD31/PECAM-1, activated EGFR, activated VEGFR-2, activated MAPK, and activated AKT; TUNEL and double staining (CD31/TUNEL, CD31/ActEGFR, and CD31/ActVEGFR-2) were also performed. The tissues were sectioned (8 to 10 μm), mounted on positively charged Plus slides (Fisher Scientific Co.), and air-dried for 30 minutes. Frozen sections were fixed in cold acetone (5 minutes), 1:1 acetone/chloroform (v/v; 5 minutes), and acetone (5 minutes) and washed with PBS. Immunohistochemical procedures were performed as described previously (20). A positive reaction was visualized by incubating the slides with stable 3,3′-diaminobenzidine for 10 to 20 minutes for CD31/PECAM-1 and all paraffin slides. The sections were rinsed with distilled water, counterstained with Gill's hematoxylin for 1 minute, and mounted with Universal Mount (Research Genetics). A positive reaction for activated EGFR and activated VEGFR was visualized by incubating the slides for 1 hour with a 1:400 dilution of Alexa Fluor 488-conjugated goat antirabbit IgG at room temperature for 1 hour in the dark. For activated MAPK and activated AKT, a 1:600 dilution of Alexa Fluor 594-conjugated goat antirabbit IgG was used. Fluorescent bleaching was minimized by covering the slides with a mixture of 90% glycerol and 10% PBS. Control samples exposed to the secondary antibody alone showed no specific staining.

TUNEL assay was performed using an apoptosis detection kit (Promega) with the following modifications: samples were fixed with 4% paraformaldehyde (methanol-free) for 10 minutes at room temperature, washed twice with PBS for 5 minutes, and then incubated with 0.2% Triton X-100 for 15 minutes at room temperature. After two 5-minute washes with PBS, the samples were incubated with equilibration buffer for 10 minutes at room temperature. The equilibration buffer was drained, and the reaction buffer containing 44 μL of equilibration buffer, 5 μL of nucleotide mix, and 1 μL of terminal deoxynucleotidyl transferase (Promega kit) was added to the tissue sections and incubated in a humid atmosphere at 37°C for 1 hour, avoiding exposure to light. The reaction was terminated by immersing the samples in 2× SSC for 15 minutes.

Samples were then washed three times for 5 minutes to remove unincorporated fluorescein-dUTP.

For quantification of endothelial cells, the samples were incubated with 1 μg/mL Hoechst stain for 2 minutes at room temperature. Fluorescent bleaching was minimized by treating slides with glycerol/PBS mounting medium containing 0.1 mol/L propyl gallate. Immunofluorescence microscopy was done with a $\times$100 objective on an epifluorescence microscope equipped with narrow band pass excitation filters mounted on a filter wheel (Ludl Electronic Products, Hawthorne, NY) to individually select for green, red, and blue fluorescence. Images were captured with a three-chip camera (Sony Corporation of America, Montvale, NJ) mounted on a universal microscope (Carl Zeiss, Tohnwood, NY) and Optimas image analysis software (Bioscan, Edmond, WA) installed on a Compaq computer with a Pentium chip, a frame grabber, an optical disk storage system, and a Mavigraph UP-D7000 digital color printer (Sony, Tokyo, Japan). To produce prints, images were additionally processed with Adobe PhotoShop software (Adobe Systems, Mountain View, CA). Endothelial cells were identified by red fluorescence, and DNA fragmentation was detected by localized green and yellow fluorescence within the nuclei of apoptotic cells.

For the quantification analysis, five slides were prepared for each group, and two areas were selected in each slide. The percentage of stained cells among the total number of cells in each area and the average proportion of stained cells in each group were calculated and compared. For total TUNEL and PCNA expression, the cells were counted in 10 random 0.159-mm^2 fields at $\times$100 magnification. Quantification of apoptotic endothelial cells was expressed as an average of the ratio of apoptotic endothelial cells to the total number of endothelial cells in 10 random 0.011-mm^2 fields at $\times$400 magnification. To quantify microvessel density (MVD), 10 random 0.159-mm^2 fields at $\times$100 magnification were captured for each tumor, and microvessels were quantified as described previously (21, 22).

Statistical Analysis. The Wilcoxon nonparametric test was used to test for differences in mice tumor volume and mice weight between each treatment group and control group on each day. To statistically model treatment, time, and treatment-by-time interactions on mouse tumor volume and mouse weight over the treatment period, a generalized linear mixed model was used. Because half of the mice in the control group had to be killed and the missing values did not appear at random, only the data before 21 days were used in the analysis in all experimental models. Survival was analyzed with the Kaplan-Meier method. Differences between treatment and control groups were compared with the log-rank test. To test for differences of quantitative immunohistochemical analyses between treatment groups, a mixed model was used. Student's *t* test from the mixed model was used to assess between-treatment differences. The linear mixed model with a compound symmetric correlation matrix was used to adjust for within-slide correlation (23).

RESULTS

AEE788 Inhibits *In vitro* Proliferation of SCCHN Cells and Sensitizes Them to Paclitaxel-mediated Toxicity. MTT assay was used to evaluate the effect of AEE788 on the proliferation of JMAR and MDA1986 cells. AEE788 inhibited cell growth of both cell lines, with an IC_{50} of 0.287 μmol/L for the MDA1986 cells (Fig. 1*A*) and 0.8 μmol/L for the JMAR cells (data not shown) in medium supplemented with 2% serum. Moreover, treatment of the MDA1986 cells (Fig. 1*B*) and JMAR cells (data not shown) with AEE788 increased their sensitivity to paclitaxel but did not increase the level of inhibition achieved with paclitaxel at a high concentration.

AEE788 Induces Apoptosis of SCCHN Cells and Sensitizes Them to Paclitaxel-mediated Apoptosis. To assess the effects of AEE788 on the induction of apoptosis in the oral cancer cell lines JMAR and MDA1986, the cells were incubated *in vitro* with paclitaxel in the absence or presence of AEE788 and then evaluated for apoptosis with a flow cytometry-based assay. At 48 hours after the start of treatment with AEE788 at 4.5 μmol/L (JMAR) and 5.5 μmol/L (MDA1986), respectively, the percentage of apoptotic cells in the MDA1986 cell line (Fig. 1*C*) and JMAR cell line (data not shown) was 50%. The addition of 5 μmol/L AEE788 significantly increased tumor cell death. This concentration of AEE788 decreased the concentration of paclitaxel needed to induce 50% apoptosis from 2.2 to 1.0 nmol/L in the JMAR cell line (data not shown). At 5 nmol/L concentration, paclitaxel alone induced ~45% cell death. At the same paclitaxel concentration (5 nmol/L), when 0.5 μmol/L AEE788 was added, the percentage cells undergoing apoptosis increased to 78% (Fig. 1*D*).

AEE788 Inhibits EGF-induced EGFR, VEGFR, MAPK, and AKT Phosphorylation in SCCHN Cells. To determine whether AEE788 could inhibit EGFR-stimulated growth and survival signaling pathways of MDA1986 and JMAR cells, the cells were stimulated *in vitro* with EGF and then treated for 1 hour with AEE788 at various concentrations. Cell lysis and Western blotting for phosphorylated forms of EGFR, VEGFR-2, AKT, and MAPK revealed inhibition of phosphorylation of all four of these kinases at 0.1 μmol/L and complete inhibition of the activity of these kinases at 2 μmol/L. Total levels of EGFR and AKT remained unchanged by AEE788 treatment (Fig. 2). Results were similar in the JMAR cells using slightly higher concentrations of AEE788 (data not shown).

AEE788 Inhibits the Growth of Orthotopic SCCHN and Prolongs Survival in Nude Mice. To assess the effects of AEE788 on *in vivo* tumor growth, an orthotopic nude mouse model of SCCHN was used.

As shown in Table 1, in the MDA1986 orthotopic model, the tumor volume of mice treated with AEE788 alone or in combination with paclitaxel was significantly lower than that of the mice in the control group ($P = 0.0048$ for the AEE788 group and $P = 0.0022$ for the AEE788 plus paclitaxel group at day 21). Overall, the tumor volume was significantly lower in the groups treated with AEE788 alone, paclitaxel alone, and the combination of AEE788 and paclitaxel than in the control group ($P < 0.0001$, $P = 0.0313$, and $P < 0.0001$, respectively). Mouse tumor volume increased over time.

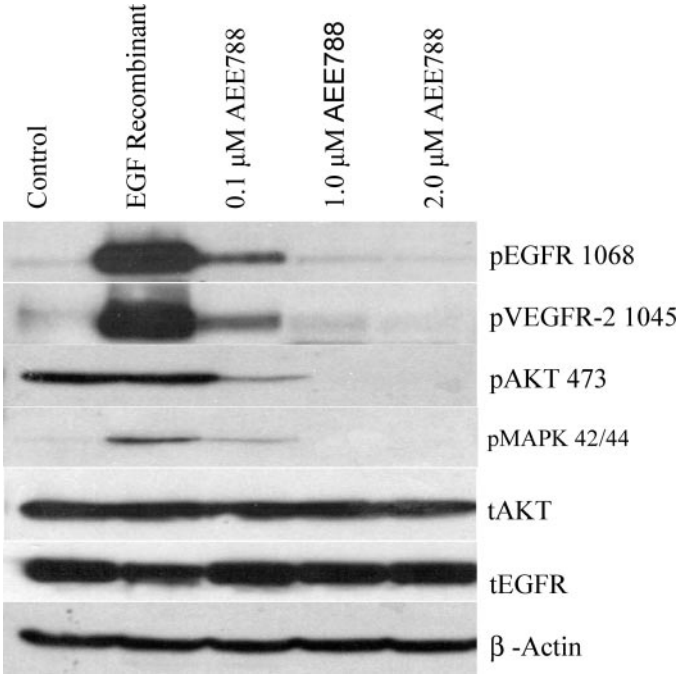

Fig. 2. Dose-dependent inhibition of EGF-induced EGFR, VEGFR, MAPK, and AKT autophosphorylation in MDA1986 oral cancer cells after treatment with AEE788. EGF-induced autophosphorylation of EGFR, VEGFR, MAPK, and AKT was evaluated in MDA1986 cells growing *in vitro* in serum-free medium that were stimulated for 15 minutes with EGF (40 ng/mL) in the presence or absence of AEE788. Western blotting was performed on protein extracts that were probed with antihuman EGFR phosphorylated at tyrosine 1068, VEGFR-2 phosphorylated at tyrosine 1045, MAPK phosphorylated at threonine 42/44, AKT phosphorylated at Ser^{473}, total AKT, and total EGFR.

Table 1 *In the MDA1986 orthotopic model, tumor volumes in mice by treatment group on observational days 7, 14, and 21*

Day	Treatment	No.	Mean	SD	Median	Minimum	Maximum	*P*
7	Paclitaxel	10	11.811	8.450	7.322	4.184	25.627	0.75
	AEE788	10	10.192	6.951	8.172	4.184	25.627	0.95
	AEE788 + paclitaxel	10	11.833	7.488	10.624	4.184	25.627	0.88
	Control (HBSS)	10	11.838	8.643	9.676	2.940	25.627	
14	Paclitaxel	10	45.382	42.262	28.242	13.075	128.135	0.16
	AEE788	10	16.030	5.470	15.298	9.806	23.535	0.0005
	AEE788 + paclitaxel	10	11.214	5.418	9.806	5.230	20.351	0.0002
	Control (HBSS)	10	50.568	29.858	45.370	18.828	128.135	
21	Paclitaxel	5	74.674	30.603	80.366	33.572	108.522	0.46
	AEE788	10	35.264	14.391	34.278	10.460	61.455	0.0048
	AEE788 + paclitaxel	10	15.686	8.145	13.778	5.822	36.250	0.0022
	Control (HBSS)	5	114.663	94.152	65.758	58.576	278.706	

Similarly, in the JMAR orthotopic model, tumor volume was significantly lower in the combination-treated group than in the control group after day 14 ($P = 0.0006$ for day 21). After day 17, compared with the control group, the AEE788-treated group had significantly lower tumor volume ($P = 0.0016$ for day 21); at day 21, the paclitaxel group also showed significantly lower tumor volume ($P = 0.0548$; table not shown).

Overall, the groups receiving AEE788 alone or in combination with paclitaxel had significantly lower tumor volumes than did the control group ($P < 0.001$ for both study groups).

Two of the 10 mice in each of the combination treatment groups for both the JMAR and the MDA1986 orthotopic tongue models had no histologic evidence of tumors at the end of the study.

In the JMAR orthotopic model, the survival rate differed significantly between the treatment groups and the control group (all $P < 0.05$). Compared with the control group, mice treated with AEE788, paclitaxel, or the combination of AEE788 and paclitaxel had significantly increased survival rates, with *P* values of 0.0029, 0.0403, and 0.0009, respectively.

In the MDA1986 orthotopic model, the survival rate of the mice treated with AEE788 alone or in combination with paclitaxel was significantly greater than that of the mice in the control group ($P < 0.0001$ for both study groups; Fig. 3). There was no significant difference in survival rates between the group treated with paclitaxel alone and the control group.

Immunohistochemical Analyses. The results of immunohistochemical analysis showed that tumors from mice in all four treatment groups expressed similar levels of EGF, VEGF, EGFR, and VEGFR. Tumors from mice treated with AEE788 alone or the combination of AEE788 plus paclitaxel had decreased levels of staining for activated EGFR, activated VEGFR, activated AKT, and activated MAPK compared with the control and paclitaxel-treated groups. In addition, tumors from mice treated with AEE788 or combination therapy had decreased MVD, decreased PCNA levels, and increased TUNEL-positive cells. Double staining for CD31/TUNEL was performed with CD31 (red staining) and TUNEL (green staining). The percentage of apoptotic endothelial cells (yellow staining) was increased in the tumors from mice treated with AEE788 or AEE788 plus paclitaxel. Moreover, double staining for CD31/Act-EGFR and CD31/Act-VEGFR, which were performed with CD31 (red staining) and Act-EGFR and Act-VEGFR (green staining), revealed that only tumors from mice treated with AEE788 and AEE788 plus paclitaxel had decreased double staining for these markers, a finding consistent with decreased signaling through EGFR and VEGFR in endothelial cells (Fig. 4).

Quantitative immunohistochemical analyses were carried out to

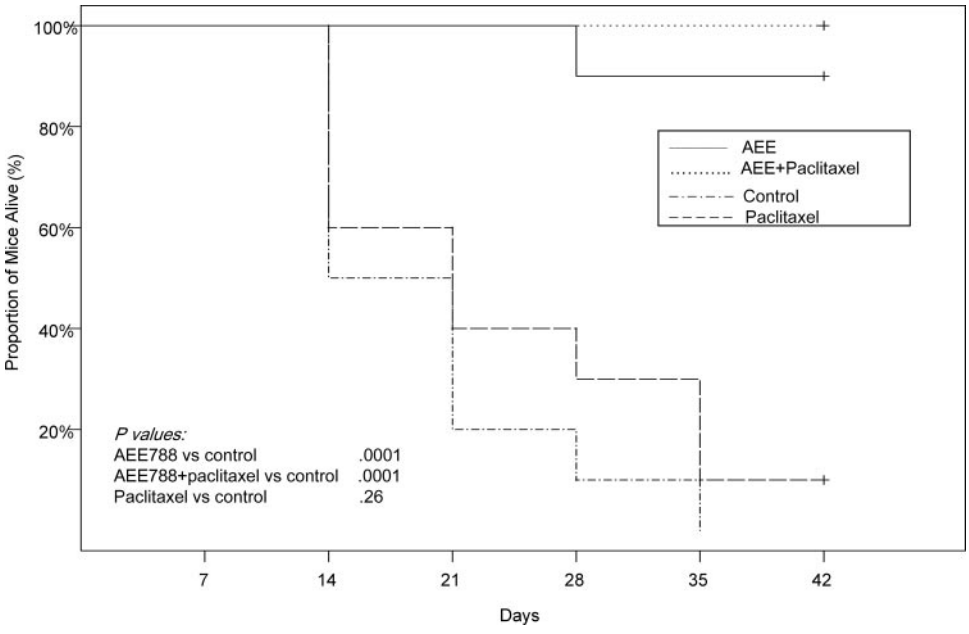

Fig. 3. Prolonged survival in an orthotopic nude mouse oral cancer model after treatment with AEE788 alone or in combination with paclitaxel. MDA1986 oral cancer cells were implanted into the tongues of nude mice. After lingual tumors developed, mice were randomized into four groups ($n = 10$ mice/group): the control group received oral diluent (90% polyethylene glycol 300 + 10% 1-methyl-2-pyrrolidinone) and i.p. HBSS; group 2 received once-weekly i.p. injections of paclitaxel (200 μg/week); group 3 received AEE788 three times weekly by oral administration (50 mg/kg); and group 4 received AEE788 in combination with paclitaxel (three-times-weekly oral AEE788 and once-weekly paclitaxel). Most of the control and paclitaxel mice had to be sacrificed before the 35th and 42nd day, respectively, but only one mouse in the AEE group had to be sacrificed before those dates. The rest of the mice of the AEE group and all of the mice in the combination group were sacrificed at the 42nd day. AEE788 alone or in combination with paclitaxel had significantly increased the survival rate as compared with the control group ($P < 0.0001$ for both study groups).

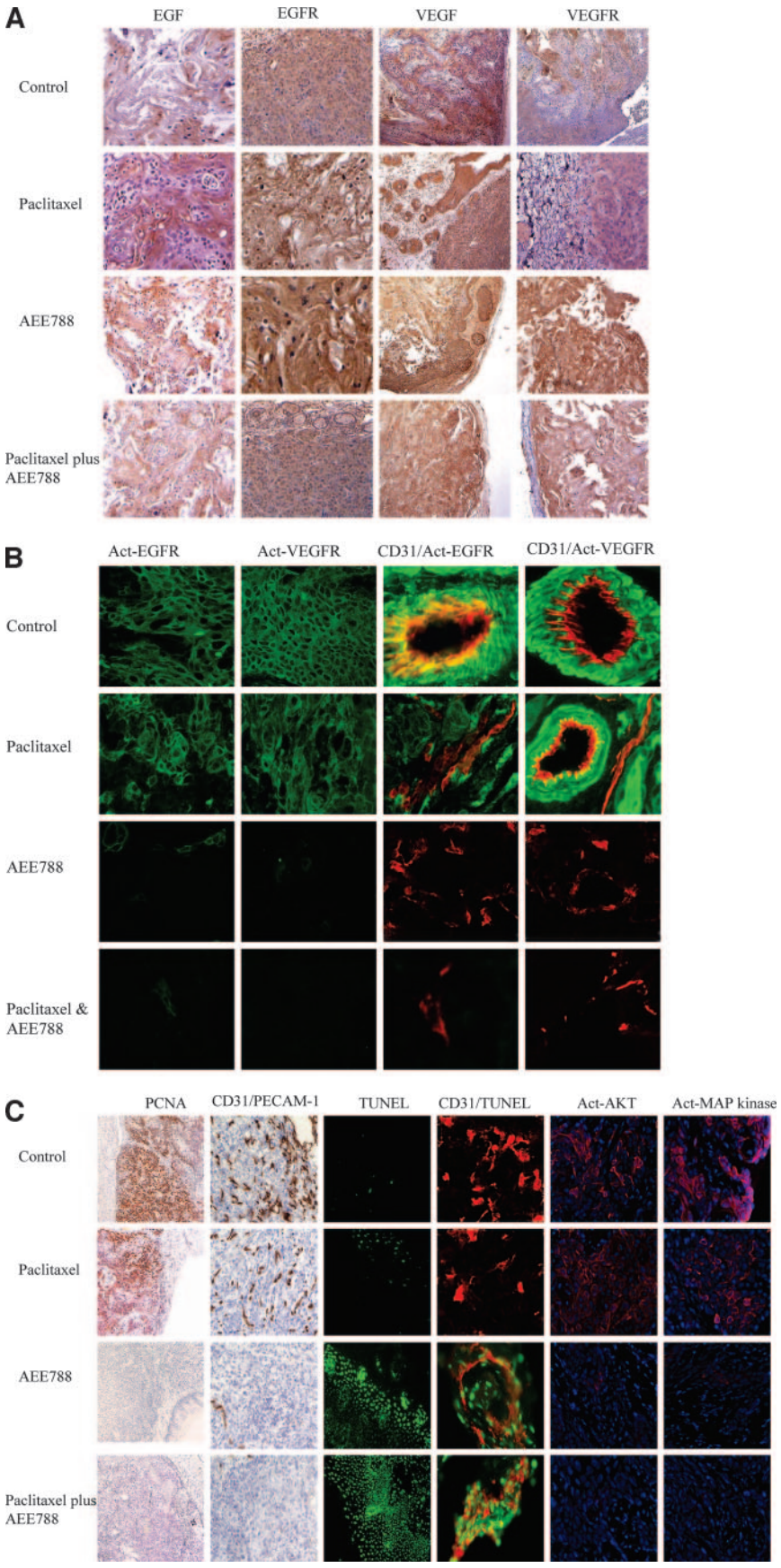

Fig. 4. Inhibition of receptor and downstream-kinase phosphorylation and increase in tumor and endothelial apoptosis after treatment of oral cancer-bearing mice with AEE788 with or without paclitaxel. Tumors arising from MDA1986 cells that had been injected into nude mice were harvested and processed for histologic and immunohistochemical analyses 42 days after treatment with once-weekly i.p. injections of paclitaxel (200 μg/week), three-times-weekly oral administration of AEE788 (50 mg/kg), or a combination of both regimens, or HBSS (control). *A*. Immunohistochemical analysis with specific anti-EGF, anti-VEGF, anti-EGFR, and anti-VEGFR antibodies showed that tumors from all four treatment groups expressed similar levels of EGF, EGFR, VEGF, and VEGFR. *B*. Specific antibodies directed against tyrosine-phosphorylated activated EGFR and activated VEGFR were used to assess phosphorylation cascades. The tumors from mice treated with AEE788 alone or in combination with paclitaxel showed decreased phosphorylated activity of EGFR and VEGFR. Also, double staining for CD31/Act-EGFR and CD31/Act-VEGFR was performed with CD31 (*red* staining) and Act-EGFR and Act-VEGFR (*green* staining). *C*. Tumors were stained for PCNA, CD31/PECAM-1, TUNEL, CD31/TUNEL, activated AKT, and activated MAPK. Tumors from mice treated with AEE788 alone or in combination with paclitaxel had decreased expression of PCNA (decreased tumor cell proliferation) and CD31/PECAM-1 (decreased microvessel density), as well as increased apoptosis as determined by TUNEL. Double staining for CD31/TUNEL was performed with CD31 (*red* staining) and TUNEL (*green* staining). Apoptotic endothelial cells (*yellow* staining) was increased in the tumors treated with AEE788 alone or in combination with paclitaxel.

Table 2 *Quantitative immunohistochemical analysis of MDA1986 tumors in tongues of nude mice*

Treatment group *	Tumor cells		Endothelial cells	
	PCNA †	TUNEL †	CD-31 †	TUNEL ‡
Control (HBSS)	19.04 ± 3.02	5.17 ± 4.06	11.92 ± 4.87	1.1 ± 0.99
Paclitaxel alone	16.69 ± 2.98	11.20 ± 7.37	7.90 ± 2.57	2 ± 1.05
AEE788 alone	4.52 ± 2.16 §	38.36 ± 10.59 §	1.17 ± 0.94 §	12.60 ± 3.47 §
AEE788 + paclitaxel	3.78 ± 2.44 §	48.58 ± 12.09 §	0.58 ± 0.49 §	16.1 ± 3.81 §

* MDA1986 tumors injected into nude mice were harvested and processed for histologic and immunohistochemical analyses 42 days after treatment with once-weekly i.p. injections of paclitaxel (200 μg/week), three-times-weekly oral administration of AEE788 (50 mg/kg), a combination of both drugs, or HBSS used as a control.

† Mean ± SD, ratio of positive cells/total cells determined from measurement of 10 random 0.159-mm^2 fields at ×100 magnification.

‡ Median of the ratio of apoptotic endothelial cells to total number of endothelial cells in 10 random 0.011-mm^2 fields at ×400 magnification.

§ $P < 0.001$ as compared with controls.

determine the expression of PCNA, and TUNEL, CD31, and double staining of CD31/TUNEL in the specimens from orthotopic models were performed. The percentages of PCNA-positive cells were lowest in the tumors from mice treated with AEE788 alone or in combination with paclitaxel. In the TUNEL assay, the fraction of apoptotic cells in tumor specimens from the mice treated with AEE788 alone or in combination with paclitaxel was greater than that in the placebo-treated mice. These *in vivo* data closely correlate with the *in vitro* results (measured by PI assay). As a measure of tumor MVD, tumors were stained with antibodies directed against CD31. Compared with specimens from the control-treated mice, tumor specimens from mice treated with AEE788 alone or in combination with paclitaxel had significantly lower tumor MVD ($P < 0.0001$). Double-labeling immunohistochemical analysis using fluorescent antibodies against CD31 (*red*) and TUNEL (*green*) revealed a progressive increase in the percentage of apoptotic endothelial cells in the tumors treated with AEE788 alone or in combination with paclitaxel (Table 2). Therefore, AEE788 reduced MVD and increased apoptosis *in vivo*.

DISCUSSION

AEE788 effectively inhibits cellular proliferation of head and neck cancer *in vitro* and *in vivo*. Used alone or in combination with paclitaxel, AEE788 induces tumor and endothelial cell apoptosis and is well tolerated in mice, providing a plausible basis for considering patients with head and neck cancer for clinical trials of AEE788.

EGFR elicits multiple biological effects in cells that overexpress the receptor, including proliferation, inhibition of apoptosis, invasion, and transformation (24). Comprehensive data over the past 20 years strongly support the role of EGFR and its ligands in the development and progression of SCCHN (25).

Several mAbs demonstrate antitumor efficacy against SCCHN cell lines and squamous cell carcinoma xenografts in nude mice (25). Of the EGFR-specific mAbs that have been developed to date, the human-murine chimeric mAb C225 has been studied most extensively. C225 dramatically enhances the *in vitro* and *in vivo* radiosensitivity of human SCCHN tumor cells and xenografts (26–28) and may also increase the efficacy of standard chemotherapy (29). The results of phase I clinical trials of C225 (30, 31), EMD 72000 (32), and h-R3 (33) in patients with SCCHN are encouraging. A phase II trial of h-R3 and phase II and III trials of C225 in patients with SCCHN are currently under way (34).

ZD1839 (Iressa), the most widely studied of the current EGFR tyrosine kinase inhibitors, greatly inhibits the growth of squamous carcinoma cell lines and human tumor xenografts in athymic mice (35). The combination of ZD1839 with a chemotherapeutic agent such as cisplatin or paclitaxel produced remarkable antitumor efficacy both *in vitro* and *in vivo* (36). Synergistic effects were also observed when ZD1839 was combined with radiotherapy in xenograft models (37). Another widely studied EGFR tyrosine kinase inhibitor, OSI-774, also inhibited the growth of head and neck carcinoma xenografts in athymic mice (38). A promising new protein tyrosine kinase inhibitor, PKI-166, arrests the growth of oral cancer *in vitro* and reduced tumor cell proliferation in a xenograft animal model (39). CI-1033, which targets not only EGFR but also all four members of the ErbB family of growth factor receptors, inhibited growth in several human cancer cell lines and suppressed tumor growth in athymic nude mice with human squamous cell carcinoma xenografts (40).

Several of these tyrosine kinase inhibitors are currently being assessed in phase I trials. On the basis of a successful phase I trial of OSI-774 (41), this inhibitor recently was studied in a phase II trial involving patients with advanced SCCHN (42). ZD1839 demonstrated clinically significant antitumor activity in a phase II trial against head and neck cancer (43). However, two recently completed large randomized phase III studies of ZD1839 failed to demonstrate that adding ZD1839 to a standard chemotherapeutic regimen increased survival rates in patients with advanced non–small-cell lung cancer (44, 45).

Because multiple growth-controlling pathways may be altered in cancer cells, the combination of biological therapeutics targeting two or more such pathways should be tested in clinical settings to allow development of multitargeted therapies. Indeed, studies of preclinical models demonstrated that significant sustained antitumor activity can be obtained by combining anti-EGFR agents with other targeted therapy, such as inhibitors of VEGFR activity (46).

Although EGFR inhibitors can inhibit the production VEGF by tumor cells, a more potent antitumor response can be achieved through the concomitant inhibition of VEGFR. In the present study, we determined whether the simultaneous blockade of the EGFR and VEGFR signaling pathways by the novel EGFR and VEGFR tyrosine kinase inhibitor, AEE788, alone or in combination with paclitaxel could inhibit the growth of JMAR and MDA1986 cells injected into the tongues of nude mice. Our results showed that therapy with AEE788 inhibited cell growth, induced apoptosis, and reduced the phosphorylation of EGFR, VEGFR-2, AKT, and MAPK in both the JMAR and MDA1986 cell lines. Treatment with AEE788 inhibited tumor growth and prolonged survival, and immunohistochemical study revealed that treatment with AEE788 alone and in combination with paclitaxel was associated with decreased MVD, a decreased proliferative index, and increased apoptosis of tumor and endothelial cells.

Enhanced expression of VEGF is generally associated with increased neovascularization, as measured by MVD within the tumor (47). In this study, oral administration of AEE788 alone or in combination with paclitaxel significantly decreased MVD. Furthermore, only the tumors from mice treated with AEE788 alone or in combination with paclitaxel had decreased double staining for CD31/Act-EGFR and CD31/Act-VEGFR. These decreases may be attributable to inhibition of EGFR blockade given that endothelial cells within many neoplasms have been shown to express EGFR (48). Nevertheless, our immunohistochemical findings showed an inhibition of VEGFR ac-

tivity in lesions from mice treated with AEE788 alone. These findings suggest that AEE788 can also directly inhibit the VEGFR.

In summary, we report that simultaneous blockade of the EGFR and VEGFR signaling pathway by the novel PTK inhibitor AEE788 alone and in combination with paclitaxel significantly inhibits oral carcinoma in nude mice. This inhibition of tumor growth is mediated by both direct antitumor effects and antiangiogenic effects. These data support the development of AEE788 for clinical use in the treatment of patients with SCCHN.

REFERENCES

1. Boring C, Squire TS, Tong T. Cancer statistics. CA - Cancer J Clin 1992;42:19–38.
2. Vokes EE, Wechselbaum RR, Lippman SM, Hong WK. Head and neck cancer. N Engl J Med 1993;328:184–94.
3. Reis L, Eisner M, Kosary C, Hankey B, Miller BC, Edwards B. In: SEER Cancer Statistics Review, 1973–1998. Bethesda, MD: National Cancer Institute; 2001.
4. Salomon DS, Brandt R, Ciardiello F, Normanno N. Epidermal growth factor-related peptides and their receptors in human malignancies. Crit Rev Oncol Hematol 1995; 19:183–232.
5. Mendelsohn J, Baselga L. Status of epidermal growth factor receptor antagonists in the biology and treatment of cancer. J Clin Oncol 2003;14:2787–99.
6. Viloria-Petit A, Crombet T, Jothy S, et al. Acquired resistance to the antitumor activity of epidermal growth factor receptor-blocking antibodies in vivo: a role for altered tumor angiogenesis. Cancer Res 2001;61:5090–101.
7. Senger DD, Van de Water L, Brown LF, et al. Vascular permeability factor (VPF, VEGF) in tumor biology. Cancer Metastasis Rev 1993;12:303–24.
8. Ferrara N. The role of vascular endothelial growth factor in pathological angiogenesis. Breast Cancer Res. Treat 1995;36:127–37.
9. Brown LF, Berse B, Jackman RW, et al. Expression of vascular permeability factor (vascular endothelial growth factor) and its receptors in adenocarcinomas of the gastrointestinal tract. Cancer Res 1993;53:4727–35.
10. Ciardiello F, Tortora GA. Novel approach in the treatment of cancer: targeting the epidermal growth factor receptor. Clin Cancer Res 2001;7:2958–70.
11. Bruns CJ, Solorzano CC, Harbison MT, et al. Blockade of the epidermal growth factor receptor signaling by a novel tyrosine kinase inhibitor leads to apoptosis of endothelial cells and therapy of human pancreatic carcinoma. Cancer Res 2000;60: 2926–35.
12. Shaheen RM, Ahmad SA, Liu W, et al. Inhibited growth of colon cancer carcinomatosis by antibodies to vascular endothelial and epidermal growth factor receptors. Br J Cancer 2001;85:584–9.
13. Swan EA, Jasser SA, Holsinger FC, Doan DD, Bucana CD, Myers JN. Acquisition of anoikis resistance is a critical step in the progression of oral tongue cancer. Oral Oncol 2003;39:648–55.
14. Knuefermann C, Lu Y, Liu B, et al. HER2/PI-3K/Akt activation leads to a multidrug resistance in human breast adenocarcinoma cells. Oncogene 2003;22:3205–12.
15. Nicoletti I, Migliorati G, Pagliacci MC, Grignani F, Riccardi CA. Rapid and simple method for measuring thymocyte apoptosis by propidium iodide staining and flow cytometry. J Immunol Methods 1991;139:271–9.
16. Holsinger FC, Doan DD, Jasser SA, et al. EGFR blockade potentiates apoptosis mediated by paclitaxel and leads to prolonged survival in a murine model of oral cancer. Clin Cancer Res 2003;9:3183–9.
17. Myers JN, Holsinger FC, Jasser SA, Bekele BN, Fidler IJ. An orthotopic nude mouse model of oral tongue squamous cell carcinoma. Clin Cancer Res 2002;8:293–8.
18. Shi SR, Key ME, Kalra KL. Antigen retrieval in formalin-fixed, paraffin-embedded tissues: an enhancement method for immunohistochemical staining based on microwave oven heating of tissue sections. J Histochem Cytochem 1991;39:741–8.
19. Weidner N, Semple JP, Welch WR, Folkman J. Tumor angiogenesis and metastasis: correlation in invasive breast carcinoma. N Engl J Med 1991;324:1–8.
20. Rak J, Filmus J, Kerbel RS. Reciprocal paracrine interactions between tumour cells and endothelial cells: the 'angiogenesis progression' hypothesis. Eur J Cancer 1996; 32A:2438–50.
21. Yoneda J, Kuniyasu H, Crispens MA, Price JE, Bucana CD, Fidler IJ. Expression of angiogenesis-related genes and progression of human ovarian carcinomas in nude mice. J Natl Cancer Inst (Bethesda) 1988;90:447–54.
22. Radinsky R, Risin S, Fan D, et al. Level and function of epidermal growth factor receptor predict the metastatic potential of human colon carcinoma cells. Clin Cancer Res 1995;1:19–31.
23. McCulloch CE, Searle SR. Generalized, linear and mixed models. New York: John Wiley and Sons; 2001.
24. Wells A. EGFR receptor. Int J Biochem Cell Biol 1999;31:637–43.
25. Ford AC, Grandis JR. Targeting epidermal growth factor receptor in head and neck cancer. Head Neck 2003;25:67–73.
26. Harari PM. Head and neck cancer as a clinical model for molecular targeting of therapy: combining EGFR blockade with radiation. Int J Radiat Oncol Biol Phys 2001;49:427–33.
27. Huang SM, Bock JM, Harari PM. Epidermal growth factor receptor blockade with C225 modulates proliferation, apoptosis, and radiosensitivity in squamous cell carcinomas of the head and neck. Cancer Res 1999;59:1935–40.
28. Bonner JA, Raisch KP, Trummell HQ, et al. Enhanced apoptosis with combination C225/radiation treatment serves as the impetus for clinical investigation in head and neck cancers. J Clin Oncol 2000;18(21 Suppl):47S–53S.
29. Fan Z, Fan Z, Baselga J, Masui H, Mendelsohn J. Antitumor effect of anti-epidermal growth factor receptor monoclonal antibodies plus cis-diamminedichloroplatinum on well established A431 cell xenografts. Cancer Res 1993;53:4637–42.
30. Robert F, Ezekiel MP, Spencer SA, et al. Phase I study of anti-epidermal growth factor receptor antibody cetuximab in combination with radiation therapy in patients with advanced head and neck cancer. J Clin Oncol 2001;19:3234–43.
31. Herbst RS, Hong WK. IMC-C225, an anti-epidermal growth factor receptor monoclonal antibody for treatment of head and neck cancer. Semin Oncol 2002; 29(Suppl14):18–30.
32. Bier H, Hoffmann T, Hauser U, et al. Clinical trial with escalating doses of the antiepidermal growth factor receptor humanized monoclonal antibody EMD 72000 in patients with advanced squamous cell carcinoma of the larynx and hypopharynx. Cancer Chemother Pharmacol 2001;47:519–24.
33. Crombet T, Torres L, Neninger E, et al. Pharmacological evaluation of humanized anti-epidermal growth factor receptor, monoclonal antibody h-R3, in patients with advanced epithelial-derived cancer. J Immunother 2003;26:139–48.
34. Pomerantz RG, Grandis JR. The role of epidermal growth factor receptor in head and neck squamous cell carcinoma. Curr Oncol Rep 2003;5:140–6.
35. Anderson NG, Ahmad T, Chan K, Dobson R, Bundred NJ. ZD1839 (Iressa), a novel epidermal growth factor receptor (EGFR) tyrosine kinase inhibitor, potently inhibits the growth of EGFR-positive cancer cell lines with or without erbB2 overexpression. Int J Cancer 2001;94:774–82.
36. Sirotnak FM, Zakowski MF, Miller VA, Scher HI, Kris MG. Efficacy of cytotoxic agents against human tumor xenografts is markedly enhanced by coadministration of ZD1839 (Iressa), an inhibitor of EGFR tyrosine kinase. Clin Cancer Res 2000;6: 4885–92.
37. Williams KJ, Telfer BA, Stratford IJ, Wedge SR. ZD1839 ('Iressa'), a specific oral epidermal growth factor receptor-tyrosine kinase inhibitor, potentiates radiotherapy in a human colorectal cancer xenograft model. Br J Cancer 2002;86:1157–61.
38. Pollack VA, Savage DM, Baker DA, et al. Inhibition of epidermal growth factor receptor-associated tyrosine phosphorylation in human carcinomas with CP-358,774: dynamics of receptor inhibition in situ and antitumor effects in athymic mice. J Pharmacol Exp Ther 1999;291:739–48.
39. Holsinger FC, Doan DD, Jasser SA, et al. Epidermal growth factor receptor blockade potentiates apoptosis mediated by paclitaxel and leads to prolonged survival in a murine model of oral cancer. Clin Cancer Res 2003;9:3183–9.
40. Slichenmyer WJ. CI-1033, a pan-erbB tyrosine kinase inhibitor. Semin Oncol 2001;28 (Suppl 16):80–5.
41. Hidalgo M, Siu LL, Nemunaitis J, et al. Phase I and pharmacologic study of OSI-774, an epidermal growth factor receptor tyrosine kinase inhibitor, in patients with advanced solid malignancies. J Clin Oncol 2001;19:3267–79.
42. Soulieres D, Senzer NN, Vokes EE, Hidalgo M, Agarwala SS, Siu LL. Multicenter phase II study of erlotinib, an oral epidermal growth factor receptor tyrosine kinase inhibitor, in patients with recurrent or metastatic squamous cell cancer of the head and neck. J Clin Oncol 2004;22:77–85.
43. Cohen EE, Rosen F, Stadler WM, et al. Phase II trial of ZD1839 in recurrent or metastatic squamous cell carcinoma of the head and neck. J Clin Oncol 2003;21: 1980–7.
44. Giaccone G, Herbst RS, Manegold C, et al. Gefitinib in combination with gemcitabine and cisplatin in advanced non–small-cell lung cancer: a phase III trial—INTACT 1. J Clin Oncol 2004;22:777–84.
45. Herbst RS, Giaccone G, Schiller JH, et al. Gefitinib in combination with paclitaxel and carboplatin in advanced non–small-cell lung cancer: a phase III trial—INTACT 2. J Clin Oncol 2004;22:785–94.
46. Ciardiello F, Bianco R, Damiano V, et al. Antiangiogenic and antitumor activity of anti-epidermal growth factor receptor C225 monoclonal antibody in combination with vascular endothelial growth factor antisense oligonucleotide in human GEO colon cancer cells. Clin Cancer Res 2000;6:3739–47.
47. Fontanini G, Vignati S, Boldrini L, et al. Vascular endothelial growth factor is associated with neovascularization and influences progression of non-small cell lung carcinoma. Clin Cancer Res 1997;3:861–5.
48. Bohling T, Hatva E, Kujala M, Claesson-Welsh L, Alitalo K, Haltia M. Expression of growth factors and growth factor receptors in capillary hemangioblastoma. J Neuropathol Exp Neurol 1996;55:522–7.